An official publication of the International Society for Energy, Environment and Sustainability (ISEES)

Journal of Energy and Environmental Sustainability

Journal homepage : www.jees.in

Study of Interference Effects on Wind Turbine Structures

Sreeram Rajesh*, K. Shruti, Sabareesh G.R, P.N Rao

BITS Pilani, Hyderabad Campus, Hyderabad, India

ARTICLE INFO

Received : 21 June 2019
Revised : 04 September 2019
Accepted : 11 September 2019

Keywords:
Wind Turbine Structure;
Aerodynamic Interference;
Interference Factor;
Coefficient of Pressure.

ABSTRACT

In wind farms, turbine structures exist very close to each other, which usually enhances or reduces the pressure load on the surrounding structures. This phenomenon, termed as interference effect is therefore essential from a design point of view. Provisions for considering interference effects while designing of structures are inadequate in wind loading codes and standards. The present paper investigates the interference factors for two wind turbines located in close vicinity and also compares the interference factor of a wind turbine tower with similar studies on rectangular building type structure. Some critical observations made from the results of this study is the nature of variation of the interference factor for different wind incident angles when varying distances separate the structures. The wind interference factors are observed at different locations on the wind turbine tower, and an attempt is made to categorize the various trends found.

Abbreviations

1) ABL- Atmospheric Boundary Layer
2) IF – Interference Factor
3) LES - Large Eddy Simulations
4) NREL - National Renewable Energy Laboratory
5) UDF - User Defined Function
6) C_p - Coefficient of Pressure

1. Introduction

The presence of interfering structures in the vicinity can drastically affect the pressure load acting on the primary structure. Interference effect on the structure depends on factors such as terrain category, wind incident angle, geometry and orientation of the structure, the spacing between the structure, etc. Experimental studies of interference effect between buildings have been carried out by several researchers in the past [(Kim, et al., 2011), (Hui, et al., 2012), (Yu, et al., 2015)]. Studies using numerical approach on building [(Desai, et al., 2014), (Lo, et al., 2016)] and wind turbine structures has also been carried out [(Li, et al., 2015), (Toan Tran T, 2015), (Weihing, et al., 2014)]. The present study aims to investigate the interference effects of NREL Phase VI wind turbine structure. The study adopts a numerical scheme validated by [(K.Shruti, et al., 2018)] for flow over building structures. The present study attempts to extend the scheme to wind turbine structures.

The modeling of Atmospheric Boundary Layer (ABL), as well as the turbulence in the flow domain, is vital to maintain the accuracy of the simulation models. In this study, a User Defined Function (UDF) is employed for generating the ABL [(Tamura, 2015)] and Large Eddy Simulation (LES) methods [(Vengadesan & Nithiarasu, 2007), (Tamura, 2009)] are used to model the turbulence [(Kim, et al., 2011)]. During post processing, the value of pressure coefficient (C_p) is extracted at a specific height of the structure and interference factors at this height is computed. For all the cases discussed, the is extracted from Ansys Fluent module after the simulations.

Generally, in the presence of an interfering structure, Figure 2b, a wake is formed on the windward side of the principle turbine, which causes the to be lower than expected from an isolated case. The paper considers the value of at different discrete points around the structure at a height to obtain the value of Interference Factor(IF) on the wind turbine tower at incident wind angles of 0^0, 30^0, 60^0 and 90^0. Here and Y_D represent the domain height (1.8m) and height at which pressure coefficients are extracted respectively.The study considers different tandem configurations with the two turbines placed at a distance of *1.5D, 2D* and *2.5D* respectively for each case. Here *D* is the diameter of the Wind Turbine. The geometry of the domain, Figure 2a, boundary conditions, and numerical scheme adopted are discussed in the next section.

* Corresponding Author: :

Interference factor is evaluated using the following relation:

$$IF = \frac{C_P \text{ of Principal Tower in the presence of an Interfering Tower}}{C_P \text{ of Principal Tower in the absence of an Interfering Tower}} \quad (1)$$

2. Methodology

2.1. Computational Model

The configuration analyzed consists of a principal structure and an interfering structure in a tandem arrangement, see Figure 1a. The NREL Phase VI wind turbine structure, see Figure 1b, has been adopted based on a study by [(Li, et al., 2015)]. In the current investigation, a horizontal axis wind turbine is taken as the turbine structure. Horizontal axis wind turbines, in general, find broader applications in generating electricity compared to a vertical axis wind turbine. Also, usage of vertical axis turbine is limited to a smaller scale (~8-10m, [(Pagnini, et al., 2018)]).

All the geometrical parameters used in this investigation, including the size of the computational domain were adopted from experimental work carried out in [(Kim, et al., 2011)]. The dimensions of the computational domain are X_D x Y_D x Z_D= 2.52m x 1.8m x 2.2m [(Kim, et al., 2011)]. The blade configuration is adopted from [(Li, et al., 2015)] and the numerical procedure is adopted from [(K.Shruti, et al., 2018)]. The NREL Phase VI turbine has a rotor of 10m diameter and a hub height of 12m. The simulation model is scaled down to the height of the structure analyzed in [(K.Shruti, et al., 2018)]. The numerical model has a blade diameter of 0.23m and a hub height of 0.28m. As the present study also makes a comparison of the results with that of [(K.Shruti, et al., 2018)], the scale of the structure and the geometrical parameters of the computational domain has been kept same as in the mentioned reference.

While discretizing, the domain has been divided into two regions representing the interior and exterior, seeFigure 2b. The interior region of the turbine has been divided into fine unstructured mesh to adapt easily to the curved geometry of the wind turbine blades. This region has a height of 0.7m and a diameter of 0.6m. The exterior region of the turbine has been divided into a structured multizone mesh in keeping with the requirements of the LES turbulence model. The entire mesh has a minimum feature size $10^{-4}m$ and has been divided into 17.8 million elements.

2.2. Boundary Condition

The computational domain has the following boundary conditions - velocity inlet, pressure outlet, three no slip walls, one ground wall with roughness constant of 0.0005 to model the terrain under consideration and no slip walls that represents the turbine body. The medium considered is air as an ideal gas at 300 K. An ABL, and its turbulence characteristics are defined at the inlet using a UDF with parameter $\alpha=1/4$ [(Tamura, 2015)] for urban terrain category. The mean wind velocity(V) at the inlet is 8.2 m/s and turbulent intensity (I) = 20% at the hub (h = 0.28m) of the wind turbine tower, both of which are calculated using U_G = 9.393, Z_G = 0.482 and (2) and (3) respectively. The value of is fixed based on velocity being equal to 8.2 m/s at the hub height. Z_G is fixed to make the numerical and experimental velocity profile matchapproximately (see **Figure 5:** Modelled Inlet Wind Velocity Profile). The derived turbulence intensity, (3) and associated kinetic energy K (4) is also given as boundary condition parameters using a UDF at both the inlet and outlet.

$$U_Z = U_G \left(\frac{Z}{Z_G}\right)^{\alpha} \quad (2)$$

$$I = 0.1 \left(\frac{Z}{Z_G}\right)^{-\alpha-0.05} \quad (3)$$

$$k = \frac{3}{2}\left(I.U_{avg}\right)^2 \quad (4)$$

$$\varepsilon = \frac{(U^*_{ABL})^3}{K(y+y_o} \quad (5)$$

$$U^* = C_\mu^{1/4} k_p^{1/2} \quad (6)$$

$$k_s = \left(\frac{9.793}{C_{ks}}\right) y_o \quad (7)$$

Where C_μ = 0.09, K = 0.41, Y_o = 7.6585 x 10^{-6}

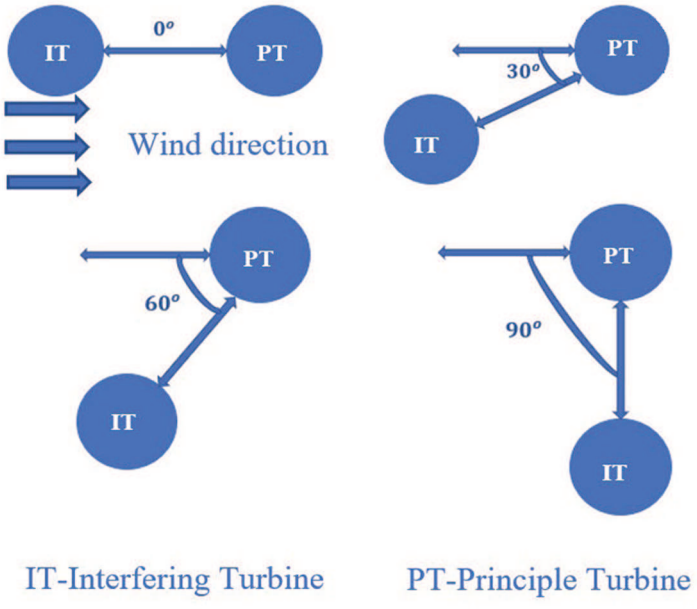

Figure 1a : Geometry of NREL Phase VI wind turbine and
Figure 1**b**: Arrangement of turbines at 0^0, 30^0, 60^0 and 90^0

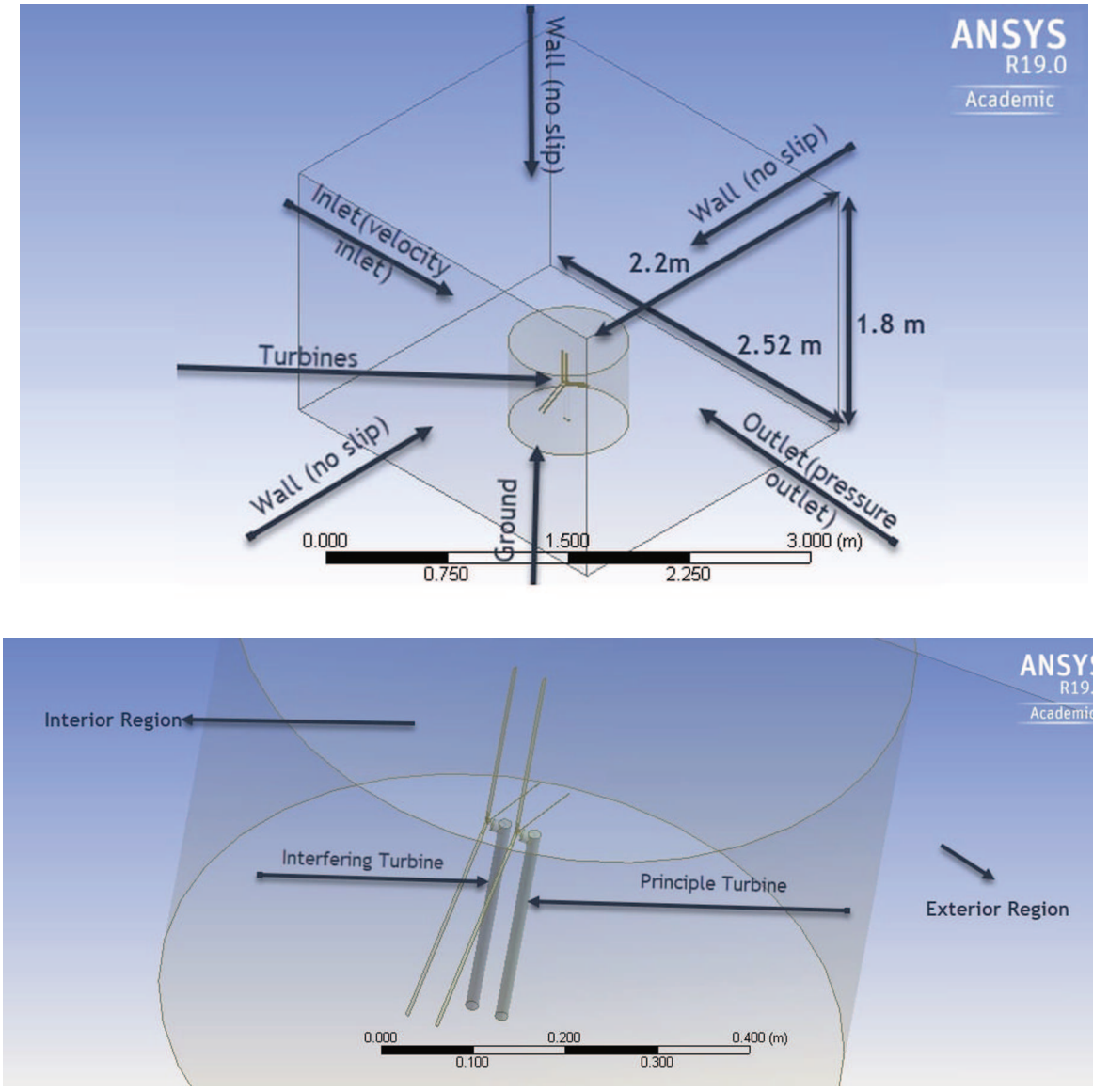

Figure 2 : a and b Geometry of the computational domain

2.3. Numerical Simulation

A transient flow with appropriate boundary conditions and a suitable turbulence model is considered to capture the fluctuations in time. The governing equation consists of filtered forms of continuity equation (8) and RANS equation which are solved using the applied boundary conditions.

The solver is initialized at the inlet. SIMPLE scheme is used for pressure velocity coupling. The kinetic energy is calculated using the power-law equation and momentum using a second-order scheme. The simulation is set under steady-state till convergence, which is observed to be less than 300 iterations for all the cases where a convergence criterion of 10^{-4} is achieved. The initial convergence is obtained through k-å turbulence model with realizable enhanced wall treatment. The converged solution is then superimposed onto a transient formulation. Turbulence model adopted for the transient formulation is LES with subgrid-scale (SGS) model to filter out eddies smaller than the minimum grid size. The Smagorinsky-Lilly SGS model without dynamic stress is used to model sub-grid turbulence (smaller eddies). The scheme used is second-order upwind with bounded second-order implicit transient formulation. The simulation is set for 150-time steps with a step size of 0.0005s, equating to a total time of 0.075s.

$$\frac{\partial \rho}{\partial t} + \frac{\partial}{\partial x_i}(\rho u_i) = 0 \tag{8}$$

$$\frac{\partial}{\partial t}(\rho u_i) + \frac{\partial}{\partial x_j}(\rho u_i u_j) = -\frac{\partial p}{\partial x_i} + \frac{\partial}{\partial x_j}\left[\mu\left(\frac{\partial u_i}{\partial x_j} + \frac{\partial u_j}{\partial x_i} - \frac{2}{3}\delta_{ij}\frac{\partial u_l}{\partial x_l}\right)\right] + \frac{\partial}{\partial x_j}\left(-\rho\overline{u_i' u_j'}\right) \tag{9}$$

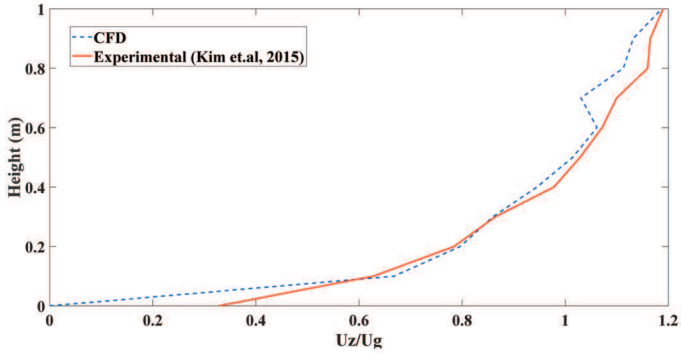

Figure 3: Modelled Inlet Wind Velocity Profile

3. Results and Discussion

3.1. Comparison between IFs for a building and wind turbine tower

The present investigation aims to understand and compare the IF between structures with comparable heights existing in a real-world environment. The IF at the height of Y_D/y - 7.5 has been evaluated on a wind turbine tower and the results are then compared to the IF of a rectangular building case at the same height.It should be noted that while the building is referred to as rectangular, the base length and height of the building are not equal. The base is a square.In the building case [(K.Shruti, et al., 2018)], the distance between two buildings were maintained at 1.5B where B is the width of the building base. The aspect ratio (height by base length) of the building structure was 4. The principle building structure was placed upstream, and the interfering building was placed downstream.In this work, the distance between the two wind turbine towers is 1.5D, D being the diameter of the tower.

In the first part of our analysis, a comparison is made with the IF values corresponding to the positive peak C_p of wind turbine and building case for different incident wind angles, (see Figure 6 : Peak IF of Building vs. 1.5D Tower against incident Wind angles). Some essential observations noted here are the drastic change in the IF of the building model at a wind incident angle of 30^0. In contrast, the IF of tower model decreases gradually with increasing wind incident angles. At 0^0 incident wind angle, the building has significantly low value of IF compared to a wind turbine. This seems plausible given the wind turbine tower has a more streamlined shape than the building, which has sharp corners and thus will experience lower wind loads in its wake than the tower. In the remaining cases, the IF values show an expected trend where the wind turbine tower suffers smaller wind loads than building because of its circular shape.

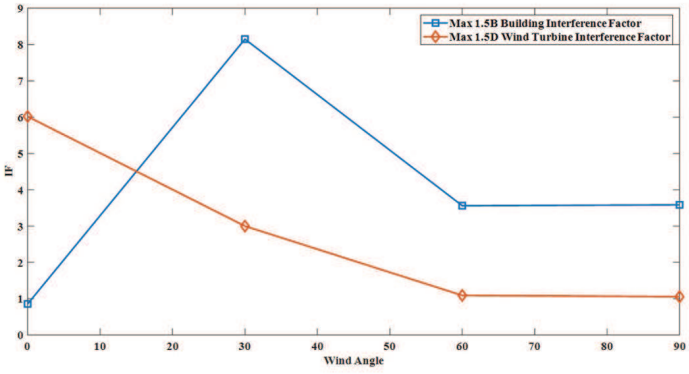

Figure 4: Peak IF of Building vs. 1.5 D Tower against incident Wind angles.

3.2. Comparison between IFs at different tandem configurations

The IFs are compared for different tandem configurations of wind turbine towers, namely 1.5D, 2D, and 2.5D at different wind incident angles, (see Figure 8: IF of the tower at 1.5D, 2D & 2.5D against incident Wind angles.). The cardinal reason for choosing the Y_D/y = 7.5 ratio is to ensure that the variation in C_p at a particular height is minimal as compared to other heights. The height ratio was therefore chosen after evaluating the at other heights.

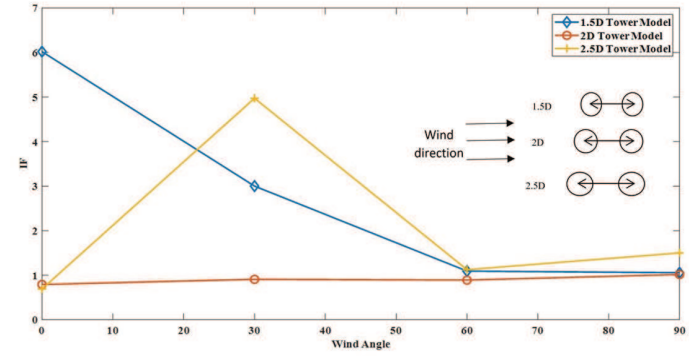

Figure 5: IF of the tower at 1.5D, 2D & 2.5D against incident Wind angles.

The IF of 1.5D tower model is observed to decrease from 6 to 1. However, in the 2.5D tower model, there is a drastic jump in the value of the IF to 5 atA possible explanation for this is due to vortex behind the interfering turbine being away from the principle turbine, as was observed in the streamline plots for the associated case. Interestingly, the IF for 2D tower model remains close to 1 throughoutand provides a desirable region with low wind loads acting on the wind turbine tower.

3.3. Comparison of IFs at different wind incident angles

The comparison of IF at discrete positions in the wind turbine case with a building case is carried out using an s/b ratio method. Here 's' is the distance along the outer edge of the structure from the front most point and 'b' is the tower diameter or building width for the respective cases, as depicted by Figure 9: s/b ratio definition forbuilding wind turbine tower respectively. The simulations were first carried out on an isolated wind turbine at incident wind angles 0^0, 30^0, 60^0 and 90^0. Then the C_p values for different s/b ratios around the wind turbine tower at a height of Y_D/y = 7.5 were extracted.

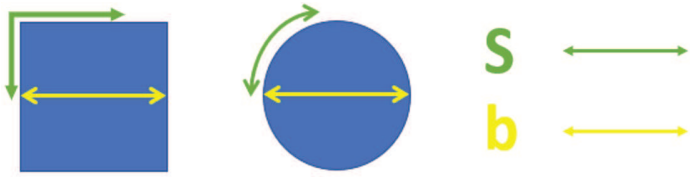

Figure 6: s/b ratio definition for building wind turbine tower respectively

For the tandem configuration in 1.5D spacing tower model, as the wind incident angle increases, the IF has a drastic jump for s/b ratios in the range 1-1.8 underwind incident angle, (see Figure11a).This indicates a drastic change in load around the principal turbine. The IF values for the 2D spacing tower model is below one throughout (see Figure 11b). Therefore, load variations are less prominent here. The 2.5D spacing tower model has the interference values below 1 for all incident wind angles except at 30^0, where the IF spikes for s/b ratios in the range 0-0.6 (see Figure11c).

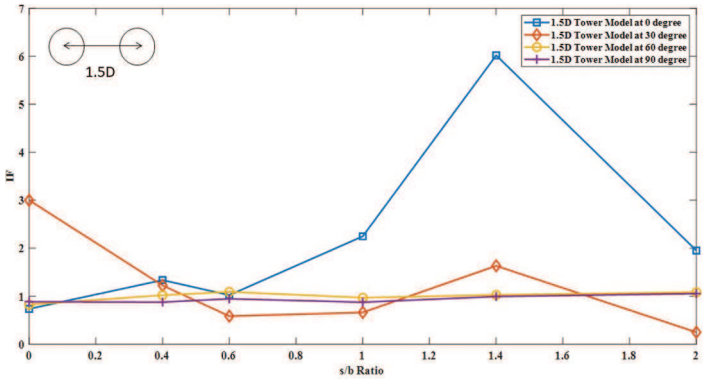

Fig. 7a

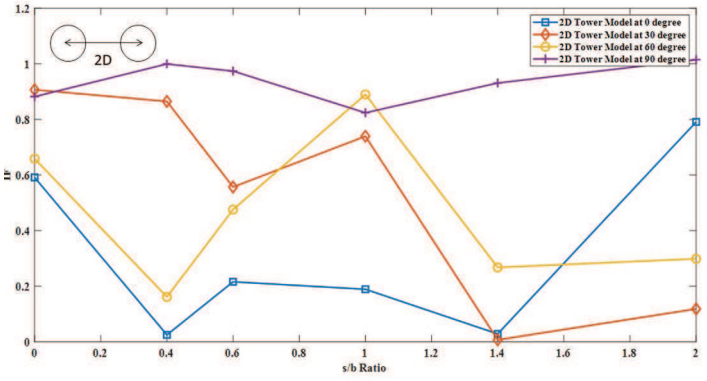

Fig. 7b

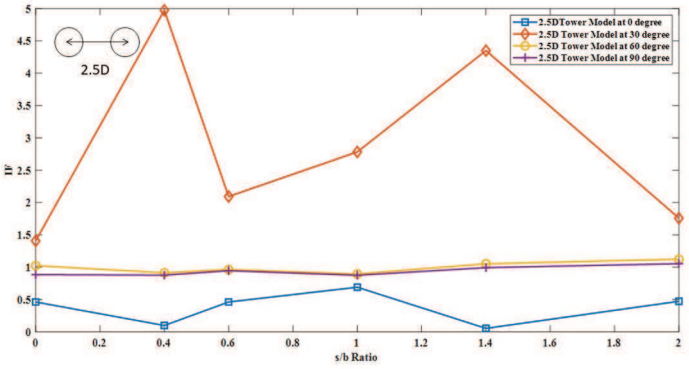

Fig. 7c

Figure7a, b and c: IF vs s/b ratio for 1.5D, 2D and 2.5D for incident wind angle 0^0, 30^0, 60^0, and 90^0

4. Conclusion

In the present paper, an attempt has been made to study the effect of two major parameters that influence the interference factor, mainly:
(a) distance between interfering structures and
(b) wind incident angle.

Some key observations made through the present numerical study includes
(1) The effect of interference becoming less prominent as the wind incident angle and the s/b ratio increases
(2) Tandem configuration of 2D yielded minimum wind loads as seen from IF values less than 1 for all wind incident angles and all s/b ratios.

References

[1] Blocken, B., Stathopoulos, T. & Carmeliet, J., 2007. CFD simulation of the atmospheric boundary layer: wall function problems. *Atmospheric Environment,* January, 41(2), pp. 238-252.

[2] Desai, A. K., Sevalia, J. K. & Vasanwala, S. A., 2014. Wind Interference Effect on Tall Building. *Wind Interference Effect on Tall Building,* Volume 8, pp. 656-662.

[3] Hui, Y., Tamura, Y. & Yoshida, A., 2012. Mutual Interference Effects between Two Building Models with Different Shapes on Local Peak Pressure Coefficients. *Journal of Wind Engineering and Industrial Aerodynamics,* Volume 104-106, pp. 98-108.

[4] K.Shruti, Sabareesh, G. R. & Rao, P. N., 2018. *Mitigating Wind Induced Disasters on a group of Buildings and Cooling Towers due to Interference Effect.* Sendai, s.n.

[5] Kim, W., Tamura, Y. & Yoshida, A., 2011. Interference effects on local peak between two buildings. *Journal of Wind Engineering and Industrial Aerodynamics,* 99(5), pp. 584-600.

[6] Li, L., Gao, L., Liu, Y. & Cui, Y., 2015. *Numerical simulation of wake interference effects on the downstream wind turbine.* Beijing, IET, pp. 1-6.

[7] Lo, Y.-L., Kim, Y. C. & Li, Y.-C., 2016. Downstream interference effect of high-rise buildings under turbulent boundary layer flow. *Journal of Wind Engineering and Industrial Aerodynamics,* December, Volume 159, pp. 19-35.

[8] Pagnini, L., Piccardo, G. & Repetto, M. P., 2018. Full scale behavior of a small size vertical axis wind turbine. *Renewable Energy,* Volume 127, pp. 41-55.

[9] Tamura, T., 2009. *Large Eddy Simulation on Building Aerodynamics.* Taipei, s.n., p. 27.

[10] Tamura, T., 2015. *Ch 6, AIJ Recommendations,* s.l.: Architectural Institute of Japan.

[11] Toan Tran T, K. D. H. N. B., 2015. Aerodynamic Interference Effect of Huge Wind Turbine Blades With Periodic Surge Motions Using Overset Grid-Based Computational Fluid Dynamics Approach. *Journal of Solar Energy Engineering,* Volume 137, p. 6.

[12] Vengadesan, S. & Nithiarasu, P., 2007. Hybrid LES — Review and assessment. *Sadhana,* April, 32(5), pp. 501-511.

[13] Weihing, P. et al., 2014. CFD Simulations on Interference Effects between Offshore Wind Turbines. *Journal of Physics: Conference Series,* June, Volume 524, p. 012143.

[14] Yu, X., Xie, Z., Zhu, J. & Gu, M., 2015. Interference effects on wind pressure distribution between two high-rise buildings. *Journal of Wind Engineering and Industrial Aerodynamics,* July, Volume 142, pp. 188-197.